Sci. Rep. RITU A41 (1996) pp. 163-169
No. 2, January 1996

Order-N Tight-Binding Molecular Dynamics: Application to Giant Fullerenes

S. Itoh [a] , P. Ordejón [b] [c] , D. A. Drabold [d] , R. M. Martin [b] [c] and S. Ihara [a]

[a] *Central Research Laboratory, Hitachi, Ltd., Tokyo 185, Japan*
[b] *Department of Physics, University of Illinois at Urbana-Champaign, Urbana, Illinois 61801*
[c] *Materials Research Laboratory, University of Illinois at Urbana-Champaign, Urbana, Illinois 61801*
[d] *Department of Physics and Astronomy, Condensed Matter and Surface Science Program, Ohio University, Athens, Ohio 45701-2979*

(Received November 14, 1995)

We present a molecular dynamics study of the energetics and structures of very large carbon cage clusters, which has been performed using tight-binding methods, both empirical and *ab initio*. The use of an order-N scheme, which provides the solution of the electronic problem with an effort proportional to the size of the system, allowed us to study carbon cage clusters with up to 3840 atoms using workstation HP755 (512MB). We have considered clusters with spherical and with toroidal topology, and systematically find that spherical clusters have lower energy than toroidal clusters of the same size. However, the toroidal C_{360} and larger clusters have lower energy per atom than the fullerene C_{60}, and therefore should be possible to be synthesized. Concerning the spherical carbon cage clusters, we show that, in all cases, their minimum energy shape is markedly polyhedral rather than spherical. The clusters present nearly flat faces between each three protruding pentagon sites. The surfaces are nevertheless smooth, without sharp edges in the lines joining the pentagons, which would be present in a perfect truncated icosahedron.

KEYWORDS: Fullerene, order-N, tight-binding, molecular dynamics

1. Introduction

After the discovery of fullerene C_{60}[1], many kinds of carbon structures have been observed experimentally. For instance, higher fullerenes, crystals of C_{60} molecules, onionlike multi-shell fullerenes[2], single wall tubes[3], polymerization of C_{60} molecules in the solids[4], and so on. In all these materials, the configuration of the polygonal network of carbon bonds and their coordinates provide important pieces of information to find out the formation mechanism and the structural properties. Since a precise experimental determination of these is often very difficult, the theoretical evaluation of the geometrical parameters is very important for an understanding of the properties of these new materials. This has become particularly evident in the study of very large, single-shell fullerene cages. The observation by Ugarte[2] of onionlike multi-shell fullerenes formed by many concentrical fullerene balls of different sizes one inside the other, has triggered the interest in the study of large single-shell fullerenes, as a preliminary step to understand the observed extremely spherical shapes of the onionlike multishell fullerenes.

Theoretical work based on elasticity theory[5, 6] as well as calculations using empirical interatomic potentials[6–8], seemed to establish that the most stable form of large single-shell fullerenes is markedly polyhedrally faceted instead of perfectly spherical. Therefore, one conclusion drawn from these studies is that the reason of the multi-shell fullerenes being spherical is not the stability of the spherical single shells, and that the intershell (van der Waals) interaction, or kinetic processes, are determinant of the experimentally observed structures. Recent *ab initio* calculations[9, 10] on large single-shell fullerenes have challenged this view, however, indicating that nearly spherical clusters may be more stable than polyhedral ones. With these results, the idea that the spherical structure of multishell clusters may be due to an intrinsic stability of the spherical single-shell fullerenes has been retaken[11].

On the other hands, a part of us have been proposed several toroidal carbon clusters[12–14] employing molecular dynamics with Stillinger-Weber (S-W) type empirical potentials[15] determined for graphite by Abraham and Batra[16]. The results indicated that those structures are energetically stable than C_{60} and could be discovered or synthesized. However, accuracy of the empirical S-W potentials is not fully sufficient to conclude definitely. In order to obtain more precise view, we have applied tight-binding method, which is more accurate than the S-W empirical potentials, to the toroidal clusters as well as the spherical clusters.

In this work, recently developed order-N method[17, 18] was employed to study the shape, structure and energetics of giant fullerenes. In these calculations, we have improved the method by using utilizing the feature of fullerenes. The Wannier functions corresponding to σ orbitals are smaller range than those for π orbitals. We found that introducing different cutoff radii for the σ and π functions can reduce the computational time while maintaining an excellent accuracy. Finally, the results are compared with those obtained from S-W empirical potentials[12–14].

2. Methodology

In this work we have applied the order-N scheme, the one developed by Mauri *et al.* and by Ordejón *et al*[18]. Our calculations are based on the tight-binding scheme. We have used two methods, which are very different in nature (one being empirical, the other *ab initio*). The first is an empirical tight-binding (ETB) model for total energies of carbon systems developed by Xu *et al.*[19] The model assumes a basis of four orbitals per C atom (one s and 3 p's), which are orthogonal (i.e., the overlap between orbitals in different atoms is taken as zero, regardless of the interatomic distance). This ETB scheme has proven useful for the study of fullerenes and other forms of carbon. However, the empirical nature of the method and the far from obvious transferability of the Hamiltonian, makes it useful to compare the results obtained with a more accurate and less *ad hoc* method. For this reason, we have also used the *ab initio* tight-binding (AITB) method of Sankey and coworkers[20]. This method is based on the LDA approximation, and uses the non-selfconsistent Harris functional, together with a minimal basis of localized, atomic like orbitals to describe the valence electrons, and pseudopotentials to eliminate the core electrons from the calculation. It is therefore a non-parameterized method, which has been extensively tested with excellent results for systems containing carbon, as well as other elements.

The carbon cage clusters which are considered here have following properties: (i) they contain only carbon atoms, (ii) there are no dangling bonds, and (iii) each atom holds covalent bonds with three neighbors. These systems therefore are formed by a σ-bonded network of atoms with sp^2 hybridization. Since there are four valence electrons in the $2s$ and $2p$ orbitals of each carbon atom, three of them form σ bonds with an electron from each of the three neighbor atoms, respectively. The remaining one electron contributes to the π orbitals of the cluster. Thus for a cluster with N carbon atoms and $4N$ electrons, $3N$ electrons occupy $3N/2$ bonds of σ-type and N electrons occupy $N/2$ bonds of π-type.

The structure of the network of σ and π bonds suggest a natural and efficient way of defining the localized functions for the order-N calculation, their center of localization and the initial guess to start the band energy minimization. We define $3N/2$ LWF's corresponding to σ-type orbitals, and $N/2$ corresponding to π-type orbitals. As initial guess for the minimization we use the bonding combination of sp^2 orbitals forming the σ bonds, and of $p_\perp$ orbitals for the π bonds. Each of the σ functions is centered in one of the $3N/2$ bonds of the cage network. The choice for the location of the π LWF's is more subtle, since there is only one π function per each pair of atoms, and therefore the choice of the center of localization is not unique. The distribution of centers must be homogeneous, in order to optimize the calculation and to ensure local charge neutrality when truncated LWF's are used. The scheme we have used here is suggested by the double-single bond structure of C_{60}: the bonds joining different pentagons are short in length, and therefore

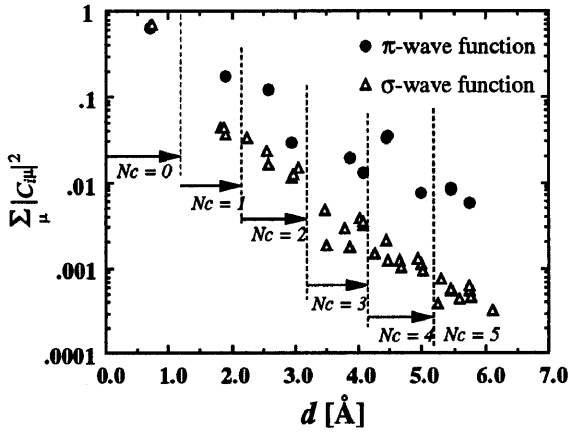

Figure 1. Decay of the localized wave function of C_{60}. σ functions (white triangles) decay much faster than π functions (black circles).

contain a π bond, whereas the bonds shared by a pentagon and a hexagon are long, single σ bonds. We can therefore assign a π LWF to each of the $N/2$ double bonds of C_{60}. For larger spherical or toroidal clusters, where the structure of double and single bonds is lost (as in graphite), we use the same construction scheme: we start assigning π functions to each of the bonds going outwards radially from the pentagons, and continue assigning π functions to bonds in alternating positions. It is easy to see that, using this procedure, the structures are covered with $N/2$ bonds of π type, in such a way that each atom forms part of just one of these bonds, ensuring that the distribution is homogeneous.

Once the centers of the localization of the LWF's are assigned as described in the previous paragraph, a localization radius must be chosen for the LWF's. Usually, a real space cutoff R_c, defined by a geometrical distance, is used to determine which atoms are included in each of the localized functions[18]. Instead, for the systems under consideration, we find it useful to use a different definition. We define the distance between an atom and the center of the LWF as the minimum integer number of bonds between the atom and the bond in which the LWF is centered. The atom is then included in the LWF if this distance is smaller than a cutoff N_c. This definition has the advantage that the number of atoms within the cutoff depends only on the topology of the bonds, and not on the curvature of the structure, and therefore on the size of the cluster.

The choice of the localization range N_c depends on the particular system under consideration. For systems with a large gap, the LWF's decay very rapidly (exponentially), so the value of N_c can be chosen to be small. For systems with a small gap, or for metals, the decay is much slower (a power law in case of metals), and larger values of N_c must be used to preserve accuracy. Fig. 1 shows the decay of the LWF's versus the distance from their center, for the spherical cluster C_{60} obtained with the ETB method with an infinite cutoff radius, The dis-

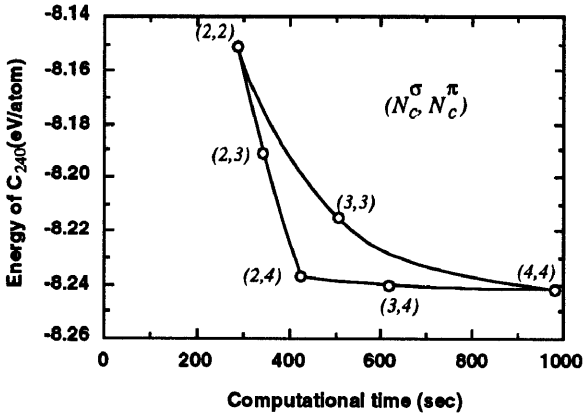

Figure 2. Energy of spherical cluster C_{240} for several different cutoff distances N_c^σ and N_c^π. Horizontal axis indicates CPU time for 1 iteration of energy minimization on SUN/Sparc-ipc.

tances corresponding to different values of the cutoff N_c are also shown in Fig. 1. As expected the LWF's decay exponentially with the distance. However, the decay is much faster for the σ-functions than for the π-functions. This characteristic is common to all carbon clusters considered, as well as to graphite. The reason is that the states in the vicinity of the energy gap are primarily π states, so their localization is weaker than for σ states. Therefore, increasing the cutoff for σ orbitals will not provide much improvement to the accuracy, while increasing the cutoff for the π orbitals will have a much larger effect. There is obviously no reason to maintain the same cutoff for both types of LWF's, and we have determined the optimum values of N_c^σ and N_c^π. We show in Fig. 2 the total energies of spherical C_{240} versus the computational time per minimization iteration for several combinations of the cutoff distances N_c^σ and N_c^π. In this figure, the lower point correspond to higher accuracy, and the points more on the left correspond to faster computation. The increase of N_c^π from 2 to 4 for the same value of $N_c^\sigma = 2$ improves the the accuracy, while not increasing the computational time much. On the other hand, increasing N_c^σ from 2 to 4 for the same distance $N_c^\pi = 4$ does not change the accuracy significantly, but increases the computational time drastically. To quantify our results, the total energies of spherical C_{60} and C_{240} calculated with the ETM model using different combinations of cutoff distances are listed in Table 1. $N_c^\sigma = 2$ and $N_c^\pi = 4$ is the most optimum set of cutoff values, providing excellent accuracy for both clusters. These results hold for the AITB method as well. In what follows, and unless specified otherwise, the results presented have been obtained using these cutoff values.

The error in the order-N solution is larger for the C_{240} cluster than for C_{60}. This is due to the closing of the gap from 1.6 eV in C_{60} to 1.1 eV in C_{240}. Increasing the cluster size further (and therefore decreasing the gap value) does not seem to further degrade the accuracy in a significant manner.

Table 1. Total energies of spherical C_{60} and C_{240} calculated by several combinations of cutoff distances.

(N_c^σ, N_c^π)	C_{60}	C_{240}
(2,2)	-7.942 (0.82%)	-8.151 (1.4 %)
(3,3)	-7.991 (0.21%)	-8.215 (0.58%)
(4,4)	-8.000 (0.10%)	-8.242 (0.25%)
(2,4)	-7.995 (0.16%)	-8.237 (0.31%)
(∞,∞)	-8.008	-8.263

3. Results and discussions

We have used molecular dynamics techniques to obtain minimum energy structures of spherical and toroidal fullerenes. In general, we used structures optimized with Stillinger-Weber potentials as initial coordinates. These where then relaxed using our order-N tight-binding method. The relaxations were performed using a dynamical quenching algorithm, either with Newtonian or with first-order equations of motion. The optimization continues until the maximum force is smaller than 0.04 eV/Å[21]. This procedure does not warranty that the obtained structures are the absolute minimum energy structures, but rather local minima. However, further annealing and quenching did not produce structures with lower energies. We are therefore confident that our structures represent accurate representation of the ground states for each cluster.

3.1. Shapes of spherical clusters

In order to establish the accuracy of the ETB and AITB Hamiltonians and of the order-N algorithm used in this work, we analyze the results for the spherical fullerene C_{60}. Table 2 shows the lengths of single and double bonds of spherical cluster C_{60} obtained in our calculations, and compared to other calculations and with experimental measurement. Our results from tight-binding methods are in excellent agreement with those of LDA calculation[22] and NMR measurement[23]. In particular, the results of the ETB Hamiltonian are exactly the same as those obtained by Xu *et al.*[19] using the same Hamiltonian, but no order-N approximation. Therefore our order-N method provides excellent accuracy for structural properties.

Table 2. Bond lengths (in Å) of spherical C_{60}.

	Double bond	Single bond
present(ETB)	1.396	1.458
present(AITB)	1.400	1.449
SW[14]	1.592	1.604
TB[19]	1.396	1.458
LDA[22]	1.40	1.45
NMR[23]	1.40±0.015	1.45±0.015

The next spherical cluster we have studied is C_{240}. This cluster has been considered by several authors, which concluded that the structure is polyhedrally

Table 3. Geometric parameters (in Å) and energies per atom (in eV, referred to that of a graphite sheet) for different forms of the spherical C_{240} obtained with the AITB method. For the energies of the clusters, we show the results of the AITB Hamiltonian obtained both with exact diagonalization (under E_{exact}) and with our order-N formulation (under $E_{O(N)}$). For comparison we show the order-N results of York *et al.* (under E_{York}).

Morphology	Bonds $(b_1, b_2, b_3, b_4, b_5)$[27]	Radii (r_1, r_2, r_3)[27]	$\bar{r}(\sigma)$[28]	E_{exact}	$E_{O(N)}$	E_{York}
sph1[9]	(1.44,1.43,1.44,1.43,1.44)	(7.12,7.12,7.12)	7.120(0.000)	0.185	0.169	0.128
sph2[9]	(1.43,1.44,1.43,1.43,1.44)	(7.12,7.12,7.12)	7.120(0.000)	0.194	0.176	0.128
fac1[9]	(1.48,1.44,1.48,1.44,1.48)	(7.03,7.42,6.97)	7.098(0.188)	0.502	0.488	0.248
fac2[9]	(1.47,1.43,1.47,1.43,1.47)	(7.63,7.21,6.75)	7.085(0.367)	0.241	0.232	0.278
fac4[9]	(1.45,1.40,1.47,1.45,1.46)	(7.49,7.19,7.05)	7.195(0.180)	0.141	0.131	0.208
S_{York}[9]	(1.43,1.43,1.45,1.42,1.44)	(7.01,7.13,7.14)	7.106(0.056)	0.210	0.195	0.108
P_{York}[9]	(1.43,1.42,1.51,1.47,1.46)	(7.66,7.19,7.07)	7.247(0.244)	0.212	0.200	0.178
YO[7]	(1.43,1.38,1.45,1.42,1.43)	(7.36,7.06,6.92)	7.065(0.180)	0.122	0.111	–
This work	(1.42,1.38,1.45,1.42,1.43)	(7.32,7.06,6.94)	7.065(0.153)	0.120	0.108	–

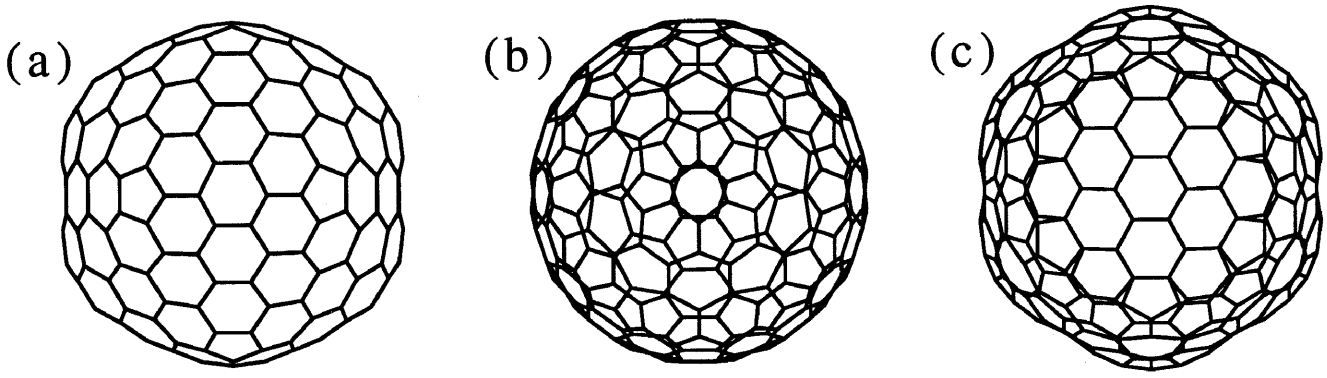

Figure 3. View of the optimized C_{240} cluster, viewed along three different axes: (a) a twofold rotation axis, (b) a fivefold rotation axis, and (c) a threefold axis.

faceted, with a significant deviation from sphericity. Yoshida and Osawa[7] and Dunlap *et al.*[24] reported structures, derived from two different empirical potentials, which were practically identical, with a standard deviation from a sphere of 0.17 Å. Adams[25] also found a faceted structure using the same AITB model as the one used in this work. Recently, however, York, Lu and Yang[9] reported results of a lower energy almost spherical structure for C_{240}. The calculations are based on a model closely related with the AITB method used here, combined with an order-N algorithm developed by Yang[10]. In their study, York *et al.* considered several different geometries as initial configurations, and relaxed the structures following a simplex algorithm (preserving the icosahedral symmetry). Two of these structures where spherical (denoted 'sph1' and 'sph2'), and three of them where faceted ('fac1', 'fac2' and 'fac4'). These relaxations yielded two different structures: an almost spherical structure 'S_{York}' with lower energy, and a polyhedral structure 'P_{York}' higher in energy by 0.07 eV/atom. The parameters defining the initial and final structures and their energies as calculated by York *et al.* are summarized in Table 3. The main result of their calculation is that the spherical clusters always have lower energy than polyhedral clusters, in contrast with the results of others. In order to shed some light in this issue, we have used our AITB model with the order-N formulation to relax the C_{240} cluster. We start with the coordinates from a relaxation of the structure with SW potentials, and follow a dynamical quenching algorithm described above. From this calculations, we obtain the structure which is shown in Figure 3.

The parameters defining the structure are shown in the last row of Table 3. We see that the optimized structure for the C_{240} cluster is significantly faceted, with a standard deviation from sphericity of 0.153 Å. This result seems to confirm the results of empirical potentials calculations, and are in disagreement with the findings of York *et al.* In order to check that our structural minimization was indeed converged to the most stable structure for the C_{240} cluster, we have also calculated the energy of all the structures considered by York *et al.* The results are also shown in Table 3. We see that our optimized structure is significantly lower in energy than the rest of the structures considered, including the minima found by York *et al.* Only the polyhedral structure proposed by Yoshida and Osawa[7], which is very similar to our optimized structure, is energetically comparable

Table 4. Average($\bar{r}$) and standard deviation(σ) of radii and planarity $\phi = 360° - (\theta_1 + \theta_2 + \theta_3)$ around pentagons in the spherical clusters. SW, ETB, and AITB indicate Stillinger-Weber potential, tight-binding method, and *ab initio* method to obtain the structures, respectively.

	$\bar{r}(\sigma, \sigma/\bar{r})$			ϕ		
size	SW	ETB	AITB	SW	ETB	AITB
C_{240}	7.86(0.29, 0.037)	7.06(0.17, 0.025)	7.06(0.15, 0.021)	13.16	8.92	7.88
C_{540}	11.75(0.46, 0.040)	10.53(0.36, 0.034)	10.53(0.35, 0.033)	13.13	9.92	9.19
C_{960}	15.64(0.64, 0.041)	14.02(0.53, 0.038)	14.01(0.52, 0.037)	13.11	9.95	9.28
C_{2160}	21.65(1.18, 0.054)	20.95(0.82, 0.039)	20.95(0.82, 0.039)	13.10	10.05	9.31
C_{3840}	29.13(1.68, 0.058)	27.95(1.08, 0.039)	-	13.07	10.05	-

to it. It is interesting to see that even the ordering of energies is very different for our results and those of York *et al.* In order to check that our order-N results are genuine, and not an artifact of the order-N approximation, we have computed the exact energy (within the AITB Hamiltonian) using diagonalization for all the structures. We see in Table 3 that the energy ordering is the same as the one obtained in the order-N calculation (in particular, our optimized structure is still the minimum energy structure). The difference between the exact and the order-N results seems to be a shift of about 0.01 – 0.02 eV. Most of this error comes from the fact that the accuracy of the order-N method for graphite is slightly different than for the fullerenes, since the gap of graphite is zero. We conclude therefore that our order-N results are accurate, and describe properly the energetics of the C_{240} cluster, within the AITB model utilized.

We have performed similar calculations for larger spherical fullerenes, using both the ETB and the AITB models. We have considered the clusters C_{240}, C_{540}, C_{960}, C_{2160} and C_{3840}. For all the cases (except for C_{3840}, which was computed only with the ETB model) minimum energy structures were obtained using both Hamiltonians. The general result is that, for all sizes and with both models, the clusters are markedly polyhedral, with a larger deviation from sphericity for the larger clusters. We show in Table 4 the average radius and the standard deviation from sphericity for all the clusters, computed for the optimum geometries obtained with SW potentials and with the ETB and AITB models. The agreement between ETB and AITB is almost perfect, and confirms that the ETB model of Xu *et al.* is an excellent Hamiltonian for these systems. We see that, although the clusters are polyhedral, with flat facets between the protruding pentagons, the edges joining the pentagonal sites are not sharp, but rounded, in order to minimize the bending energy.

Recently, Lu and Yang[26] performed an study of large fullerene balls, similar to the one reported here. They used the same method as the one used by York *et al.* for the study of C_{240}, and obtained qualitatively similar results for the larger clusters: large, isolated clusters were predicted to be spherical, in contrast with our results. Based on their results, Lu and Yang explained the experimental observation of spherical, multishell fullerenes[2], as a consequence of the stability of spherical single-shell fullerenes. Our results contradict these arguments, and suggest that there must be a different mechanism (like intershell interactions) to explain the stability of spherical multishell fullerenes.

The results of Table 4 indicate that, as a general result, the optimum structures of large fullerene balls are polyhedral, with a larger deviation from sphericity for larger sizes. The ratio of deviation to average radius of the cluster saturates, however, for about 2160 atoms. This seems to indicate that these clusters have reached the asymptotic large size regime, and increasing the size roughly preserves the shape of the cluster, with rescaled dimensions. Another measure of the non-sphericity is provided by the amount of non-planarity of the surface at the pentagonal sites. In the polyhedral structures the pentagons are protruding, and therefore there is a large deviation from planarity at those sites. Following York *et al.*[26] we define the planarity at an atom by the angle $\phi \equiv 360° - (\theta_1 + \theta_2 + \theta_3)$, where θ_1, θ_2 and θ_3 are the angles formed by the three σ bonds between the atom and its three nearest neighbors. Therefore, $\phi = 0°$ for a planar site. We show in Table 4 the results of the planarity angle ϕ for atoms in the pentagons, for all the clusters from C_{240} to C_{3840}. We see that, as observed in the deviation from sphericity, the planarity at pentagonal sites approaches a constant value for the larger clusters, again indicating that the asymptotic region has been reached. It is interesting to observe that the quantum-mechanical results, both with the ETB and the AITB models, predict a behavior which is qualitatively different from the results of Stillinger-Weber potentials. Whereas the increase in the ratio $\sigma/\bar{r}$ is observed all cases, the SW potentials predict a decrease in the non-planarity at pentagonal sites with the cluster size, whereas the ETB and AITB models predict an increase for larger sizes. This indicates that, although empirical models can be appropriate to describe the main features of the clusters, the details are far from accurately described.

3.2. Shapes of toroidal clusters

We have also initiated an study of the shapes and energies of toroidal carbon clusters. Ihara and Itoh[12–14] proposed several possibilities of toroidal clusters, using molecular dynamics with SW potentials[15] determined for graphite by Abraham and Batra[16]. The negative curvature is obtained by a combination of pentagons (in

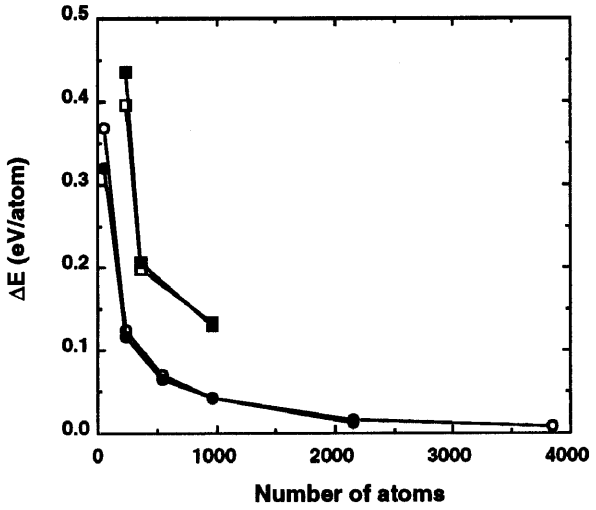

Figure 4. Total energy per atom for spherical (white circle) and toroidal (black circle) carbon cage clusters against the total number of carbon atoms.

Table 5. Total energies relative to graphite monolayer for spherical and toroidal clusters (in eV/atom). Blank boxes mean that there is no corresponding structures.

	Spherical		Toroidal	
N	ETB	AITB	ETB	AITB
60	0.3674	0.3279		
240	0.1253	0.1204	0.3962	0.4356
360			0.1995	0.2063
540	0.0693	0.0726		
960	0.0430	0.0511	0.1338	0.1299
2160	0.0166	0.0221		
3840	0.0084	–		

the outer face of the torus) and heptagons (in the inner face). Recently very similar structures have been found experimentally [29], although multi-layered and larger than the theoretically proposed structures. We have relaxed the structure of toroidal C_{240}, C_{360} and C_{960}, both with the ETB and AITB models. The tendency of the surface curvature for the toroidal clusters is very similar to that for the spherical clusters. Only the regions around the pentagons are protrusive and the planarity ϕ around the pentagons reaches the same value as that of spherical clusters.

3.3. Energies of fullerenes

We have investigated the total energy of the relaxed fullerenes as a function of their size. Figure 4 shows the total energy per atom relative to that of monolayer graphite. We show the results for the spherical and the toroidal fullerenes, obtained both with the ETB and AITB models. It is worth mentioning that there is a remarkable agreement between these two models for all the cases studied, which confirms that the simple ETB model produces a very reliable description of this kind of carbon materials. Table 5 shows the values for the relaxed spherical fullerenes, with both Hamiltonian models. The results of Figure 4 show that the spherical fullerenes are more stable than the toroidal fullerenes of the same size. The toroidal C_{240} is still less stable than icosahedral C_{60}, although larger toroidal clusters are more stable than C_{60}. These results agree with previous calculations done in the tight-binding approximation[30] and with *ab initio* self-consistent field calculations [31]. However, the toroidal C_{360} and larger clusters have lower cohesive energy than the fullerene C_{60}. Larger toroidal cage clusters are expected to be stable.

4. Conclusion

We have used molecular dynamics techniques to study the energetics and shapes of giant fullerenes. The atomic force and total energies were computed from the electronic structure, using tight-binding models. The solution of the electronic problem was obtained using a recently developed order-N method, that produces the solution with an effort that scales linearly with the size of the system, therefore allowing the calculation of systems with thousands of atoms. We have developed efficient techniques to apply these order-N methods to the specific problem of large fullerenes, by using two different cutoff distances for the σ and π wave functions. This reduces the computational time while maintaining an excellent accuracy. The results of our simulations show that, for large spherical clusters, the polyhedrally faceted shape is preferred, both for the empirical and for the *ab initio* calculations. These results contradict recent claims[9, 26], that isolated clusters may have rather spherical shapes, and rule out the possibility of an intrinsic stability of the spherical shape in single-shell clusters as the cause of the observed sphericity of onion-like multi-shell fullerenes. We have also shown that the spherical cage clusters have lower energy than toroidal cage clusters of the same size. However, the toroidal C_{360} and larger clusters have lower cohesive energies than the fullerene C_{60} and they are energetically stable. We also have studied the detailed way in which the energy of the spherical fullerenes approaches that of monolayer graphite when the size of the cluster is increased and used our computed energies to test several functional forms proposed in the literature. Implementation of our order-N method to powerfull parallel computers is straightforward and will cut the edge of the material science especially fullerene research.

Acknowledgments

Main part of this work was done by a collaboration between Hitachi and the University of Illinois. This work was partially supported by the NSF under No. DMR-89-20538 and No. DMR-93-22412, and by DOE Grant No. DEFG 02-91ER45439. Some of the computations were performed in the Convex C-3880 at the NCSA (National Center for Supercomputing Applications).

1) H. W. Kroto, J. R. Heath, S. C. O'Brien, R. F. Curl, and R. E. Smalley, Nature (London) **318**, 162

(1985); W. Krätschmer, L. D. Lamb, K. Fostriropoulos, and D. R. Huffman, *ibid.* **347**, 354 (1990).
2) D. Ugarte, Nature (London) **359**, 707 (1992); Europhys. Lett. **22**, 45 (1993).
3) S. Iijima and T. Ichihashi, Nature (London) **363**, 603 (1993);**364**, 737(E) (1993); D. S. Bethune, C. H. Klang, M. S. de Vries, G. Gorman, R. Savoy, J. Vazquez, and R. Beyers, *ibid.* **363**, 605 (1993).
4) A. M. Rao, P. Zhou, K. -A. Wang, G. T. Hanger, J. M. Holden, Y. Wang, W. -T. Lee, X. -X. Bi, P. C. Eklund, D. S. Cornett, M. A. Duncan, and I. J. Amster, Science **259**, 955 (1993).
5) T. A. Witten and H. Li, Europhys. Lett. **23**, 51 (1993).
6) J. Tersoff, Phys. Rev. B **46**, 15546 (1992).
7) M. Yoshida and E. Osawa, Fullerene Sci. Tech. **1**, 55 (1993).
8) A. Maiti, C. J. Brabec and J. Bernholc, Phys. Rev. Lett. **70**, 3023 (1993).
9) D. York, J. P. Lu, and W. Yang, phys. Rev. B **49**, 8526 (1994).
10) W. Yang, Phys. Rev. Lett. **66**, 1438 (1991).
11) D. Ugarte, MRS Bulletin, Page 39, November 1994, Volume XIX, No. 11.
12) S. Itoh, S. Ihara, and J. Kitakami, Phys. Rev. B **47**, 1703 (1993).
13) S. Ihara, S. Itoh, and J. Kitakami, Phys. Rev. B **47**, 12908 (1993).
14) S. Itoh and S. Ihara, Phys. Rev. B **48**, 8323 (1993).
15) F. H. Stillinger and T. A. Weber, Phys. Rev. B **31**, 5262 (1985); **33**, 1451(E) (1986).
16) F. F. Abraham and I. P. Batra, Surf. Sci. **209**, L125 (1989).
17) P. Ordejón, D. A. Drabold, M. P. Grumbach, and R. M. Martin, Phys. Rev. B **48**, 14646 (1993).
18) P. Ordejón, D. A. Drabold, R. M. Martin and M. P. Grumbach, Phys. Rev. B **51**, 1456 (1995).
19) C. H. Xu, C. Z. Wang, C. T. Chan, and K. M. Ho, J. Phys. Condens. Matter **4**, 6047 (1992); C. Z. Wang, C. T. Chan, and K. M. Ho, Phys. Rev. B **46**, 9761 (1992).
20) O. F. Sankey and D. J. Niklewski, Phys. Rev. B **40**, 3979 (1989).
21) In the case of the spherical C_{2160} and C_{3840}, the tolerance in the maximum force was reduced to 0.02 eV/Å. A uniform expansion or contraction of a large spherical clusters produces small atomic forces, because the stress is distributed over the surface of the sphere, with a very small strain on each bond. Therefore smaller tolerances in the forces are required for larger clusters.
22) Q. Zhang, J. -Y. Yi, and J. Bernholc, Phys. Rev. Lett. **66**, 2633 (1991).
23) C. S. Yannoni, P. P. Bernier, D. S. Bethune, G. Meijer, and J. R. Salem, J. Am. Chem. Soc. **113**, 3190 (1991).
24) B. I. Dunlap, D. W. Brenner, J. W. Mintmire, R. C. Mowrey, and C. T. White, J. Phys. Chem. **95**, 8737 (1991).
25) G. Adams, unpublished.
26) J. P. Lu and W. Yang, Phys. Rec. B **49**, 11421 (1994).
27) Inequivalent bonds and radii. See Ref. [9] for the definition.
28) Average radius and standard deviation (in parentheses).
29) S. Iijima, P. M. Ajayan, and T. Ichihashi, Phys. Rev. Lett. **69**, 3100 (1992); M. Endo, K. Takeuchi, K. Kobori, K. Takahashi, H. W. Kroto, and A. Sarkar, Carbon **33**, 873 (1995); X. F. Zhang and Z. Zhang, Phys. Rev. B **52**, 5313 (1995).
30) B. N. Davidson and J. K. Johnson, APS March meeting '94; M. R. Pederson, J. K. Johnson, and J. Q. Broughton, APS March meeting '94.
31) J. C. Greer, S. Itoh, and S. Ihara, Chem. Phys. Lett. **222**, 621 (1994).